Effect of Distribution Tabs on Mass Transfer of Artificial Kidney

Weiping Ding, Liqun He, Gang Zhao, Xiaodong Luo, and Min Zhou
Dept. of Thermal Science and Energy Engineering, University of Science and Technology of China, Hefei 230027, China

Dayong Gao
Dept. of Thermal Science and Energy Engineering, University of Science and Technology of China, Hefei 230027, China
and
Dept. of Mechanical Engineering, University of Kentucky, Lexington, KY 40506

DOI 10.1002/aic.10073
Published online in Wiley InterScience (www.interscience.wiley.com).

The configuration of the dialysate inlet and outlet is one of the main factors that affect the mass transfer performance of the artificial kidney. The effect of the distribution tabs at the dialysate inlet and outlet on mass transfer is investigated qualitatively by means of three-dimensional (3-D) flow field numerical simulation. The nonporous tabs are designed to be the porous tabs. Then the variation of the artificial kidney's clearance is studied with the porous tabs' Darcy permeability decreasing from $+\infty$ *to 0. The results show that the clearance first increases slightly, and then rises sharply; after arriving at a maximum, the clearance falls sharply and then decreases steadily. From the results, the optimal Darcy permeability of the porous tabs is found, corresponding to which the maximal clearance is about 4.5% higher than the current artificial kidney's clearance under the same conditions. The results are very significant for designers to improve the artificial kidney.*
 AIChE J, 50: 786–790, 2004
Keywords: mass transfer, distribution tab, clearance, hollow fiber, artificial kidney

Introduction

The artificial kidney has been applied to hemodialysis, and its mass-transfer performance is studied widely. There are many factors that affect mass-transfer performance of the artificial kidney. Some of the possible causes include irregularity of fiber spacing, polydispersity of fiber diameter, movement of hollow fiber during operation, influence of the module, and effects of inlet and outlet. The effects of hollow fiber distribution and packing density on mass-transfer performance have been abundantly reported in the literature (Bao et al., 1999; Costello et al., 1993; Crowder and Cussler, 1997; Noda and Gryte, 1979; Wu and Chen, 2000). However, there is little literature on the effect of the inlet and outlet configuration upon mass-transfer performance of the artificial kidney. Frank et al. (2000) measured the concentration fields within an artificial kidney using X-ray computed tomography (CT) and believed that the distribution tabs at the dialysate inlet and outlet do not produce good flow distribution.

In the current artificial kidney, there is a distribution tab at the dialysate inlet and outlet, respectively (Figures 1 and 2). The artificial kidney adopts countercurrent (that is, blood flows inside hollow fibers, whereas dialysate flows outside hollow fibers countercurrently). Transverse flow exists at the dialysate inlet and outlet. The complex inlet and outlet configuration and transverse flow cause difficulties of discussing the overall mass transfer performance theoretically. Therefore, most reports in the literature focused on the middle portion of dialyzers (Bao et al., 1999; Costello et al., 1993; Crowder and Cussler, 1997; Jaffrin et al., 1990; Noda et al., 1979). In fact, the configuration of the inlet and outlet seriously affects the velocity field within the artificial kidney, so the clearance is substantially affected.

Correspondence concerning this article should be addressed to D. Gao at dgao@engr.uky.edu.

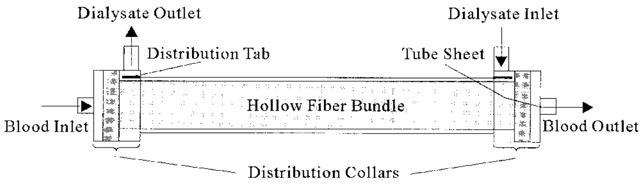

Figure 1. Typical artificial kidney module.

In this article, 3-D flow fields within the artificial kidney are determined by numerical simulation, and the effect of the dialysate inlet and outlet configuration on mass transfer is analyzed qualitatively. To the best of our knowledge, for the first time the effect of the distribution tabs at the dialysate inlet and outlet on mass transfer is investigated emphatically. The nonporous tabs are designed to be the porous tabs. Then the variation of the artificial kidney's clearance is studied with the porous tabs' Darcy permeability decreasing from $+\infty$ to 0. From the results, the optimal Darcy permeability of the porous tabs is found. The results are very significant for designers to improve the artificial kidney.

Theory

Mass transfer in the artificial kidney involves a combination of convection and diffusion, and therefore is very complex (Jaffrin et al., 1990). In this article, we assume that the blood and dialysate flows are all laminar flow, the blood and dialysate flow zones are integrated, and the hollow fiber membrane is the thin porous media that prevents blood cells from blood side to dialysate side (toxic solutes can pass freely) and increases the viscous resistance (the inertial resistance is ignored because of laminar flow). From the assumptions, we avoid complex boundary conditions and complex calculation of mass exchange between the two regions. So the control equations of the blood and dialysate sides can be described in the same form.

Continuity equation

$$\frac{\partial \rho}{\partial t} + \nabla \cdot (\rho \boldsymbol{u}) = 0 \tag{1}$$

Momentum equation

$$\frac{\partial (\rho \boldsymbol{u})}{\partial t} + \nabla \cdot (\rho \boldsymbol{u}\boldsymbol{u}) = -\nabla p + \nabla \cdot (\bar{\bar{\boldsymbol{\tau}}}) + \rho \boldsymbol{g} \tag{2}$$

Concentration equation

$$\frac{\partial (\rho C)}{\partial t} + \nabla \cdot (\rho \boldsymbol{u} C) = \nabla \cdot (\rho D \nabla C) \tag{3}$$

The hollow fiber membrane is assumed to be the thin porous media, and the control equations can be described by the following equations (Fluent 6.0).

Continuity equation

$$\frac{\partial \rho}{\partial t} + \nabla \cdot (\rho \boldsymbol{u}) = 0 \tag{4}$$

Momentum equation

$$\frac{\partial (\rho \boldsymbol{u})}{\partial t} + \nabla \cdot (\rho \boldsymbol{u}\boldsymbol{u}) = -\nabla p + \nabla \cdot (\bar{\bar{\boldsymbol{\tau}}}) + \rho \boldsymbol{g} - \frac{\mu}{\alpha} \boldsymbol{u} \tag{5}$$

Concentration equation

$$\frac{\partial (\rho C)}{\partial t} + \nabla \cdot (\rho \boldsymbol{u} C) = \nabla \cdot (\rho D \nabla C) \tag{6}$$

where stress tensor $\bar{\bar{\boldsymbol{\tau}}} = \mu[(\nabla u + \nabla u^{T})] - 2/3(\nabla \cdot u)I]$, C is the solute concentration (kg/m^3), p is the pressure (Pa), ρ is the fluid density (kg/m^3), u is the velocity tensor (m/s), g is the gravity tensor, μ is the fluid viscosity (N·s/m^2), D is the diffusivity coefficient of solute (m^2/s), and α is the Darcy permeability of the hollow fiber membrane (m^2).

Generally, the following equation is used to calculate the overall clearance

$$C_L = \frac{Q_{bi} C_{bi} - Q_{bo} C_{bo}}{C_{bi}} \tag{7}$$

where C_L is the overall clearance (mL/min); Q_{bi} and Q_{bo} are flow rates in blood inlet and outlet, respectively (mL/min); and C_{bi} and C_{bo} are solute concentration in blood inlet and outlet (kg/m^3), respectively.

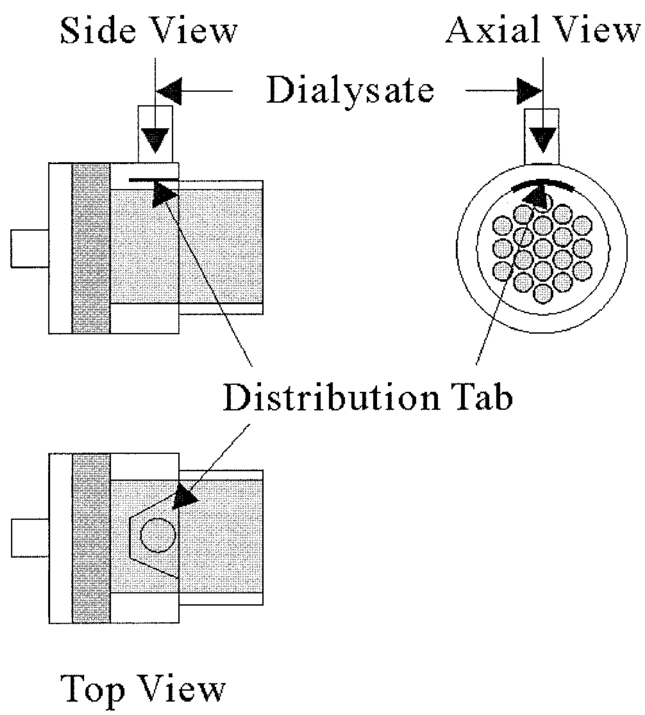

Figure 2. Geometry configuration at the dialysate inlet.

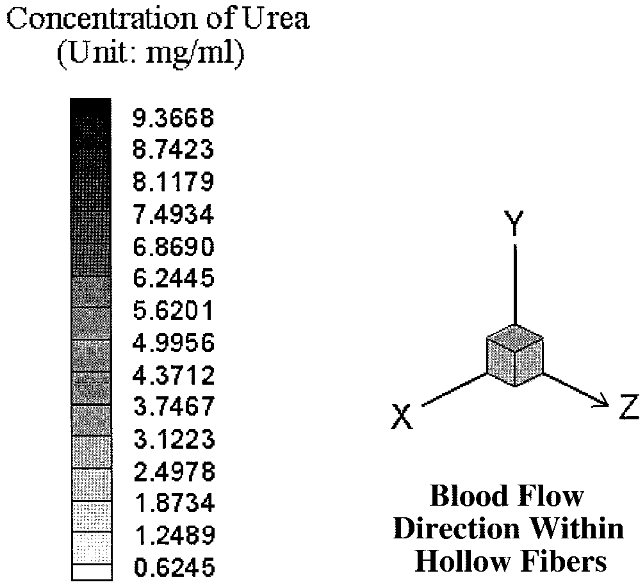

Figure 3. Urea concentration bar (left) and coordinate (right).

Simulation Computation

In this article, we only qualitatively discuss the effect of the distribution tabs on mass transfer performance. The following simulative conditions were adopted.

To reduce the number of grid nodes and improve the speed of convergence, and referring to reports of the simulation and experiment in the literature (Doleček and Cakl, 1998; Liao, 2002; Yang and Cussler, 1986), 19 hollow fibers were used in the module. The inner diameter and the outer diameter of the hollow fiber are 0.0028 and 0.0030 m, respectively. Hollow fibers were placed with a triangular array (Figure 2), and the spacing between two neighboring hollow fiber centers was 0.007 m. Other sizes referred to CT110 (Baxter Co., Bloomington, IN). Darcy permeability of the hollow fiber membrane was supposed to be 1e-09 m^2, and hollow fibers were supposed to be rigid.

The artificial kidney module was put flatly with the dialysate inlet and outlet upward. The blood was replaced by 0.85% NaCl solution with 1% urea, and the dialysate was replaced by 0.85% NaCl solution. The inlet blood flow rate and the inlet dialysate flow rate were all 400 mL/min. The blood flow direction within hollow fibers is along the positive direction of Z axis (Figure 3). The diffusivity coefficient of urea in 0.85%NaCl solution was set to be 1.82e-09 m^2/s (Klein et al., 1977). The solution properties approximatively adopted water properties at 300 K. The initial velocity and the initial concentration within the module were set to be zero, and mass-flow-inlet and pressure-outlet boundary conditions were adopted.

In our numerical simulation, the fluid software Fluent 6.0 (Lebanon Fluent Co., 2001) was used. The finite-element method discretized the above equations. The artificial kidney module was constructed and meshed using GAMBIT software. Then, the steady-state fields of pressure, velocity, and concentration were computed using Fluent 6.0 software. In the process of computing, the mesh-refinement analysis was used to increase numerical precision, and the discretization error was less than 0.2%.

Results and Discussion

In this article, the effect of the distribution tabs on mass transfer performance is acquired by studying the concentration fields within artificial kidney and clearance. Seven cross sections (that is, z values of -0.115, -0.08, -0.04, 0, 0.04, 0.08, and 0.115 m) as samples are analyzed. The small tab at the dialysate inlet can present fluid from directly impinging on the hollow fiber bundle and direct it through the distribution collar. The tab at the dialysate outlet also can direct fluid to flow around the distribution collar.

The observed variation in concentration fields suggests that the distribution tabs do not produce good dialysate flow distribution. At the dialysate inlet, because of impinging on the tab, the dialysate flows down the inner wall of the module, distributing into the space outside hollow fibers gradually. At the same time, vortexes are produced around hollow fibers and march axially. At the dialysate outlet, because of the tab, the dialysate is cumbered and has to go around the collar.

The distribution tabs cause the uneven dialysate velocity within the artificial kidney. The velocity in the lower portion of the bundle is faster than that in the upper portion, so the mass transfer is faster and the concentration of urea is lower in the lower portion, which does not benefit the overall mass transfer (Figure 4). (The higher concentration in the midportion is caused by the uneven blood velocity primarily because of the blood inlet and outlet configuration.)

To solve the problem that the distribution tabs cause the uneven dialysate flow distribution, we first attempt to remove both tabs. The results show that the higher concentration appears in the mid and lower portion of the bundle (Figure 5). In fact, because of no tabs, the dialysate flows preferentially in the portion of the fiber bundle close to the dialysate outlet (Frank

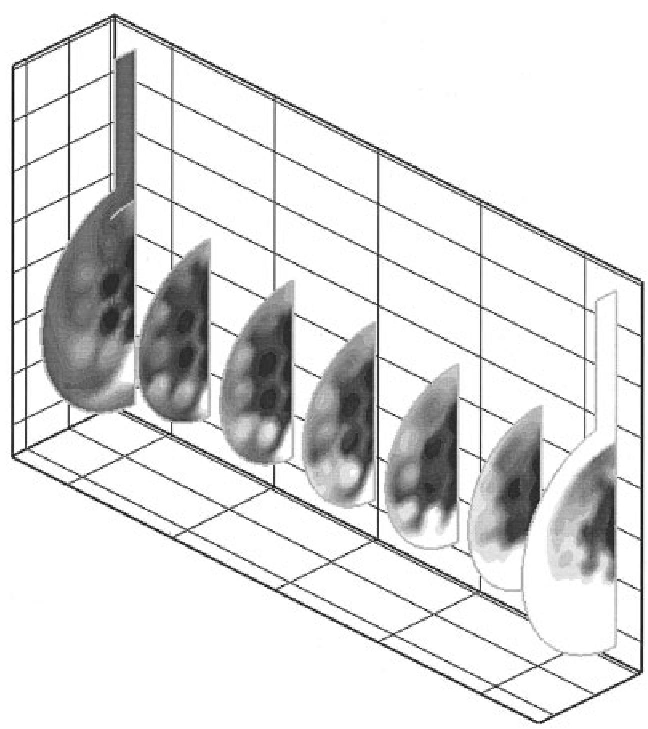

Figure 4. Concentration profiles with Darcy permeability of tabs close to 0.

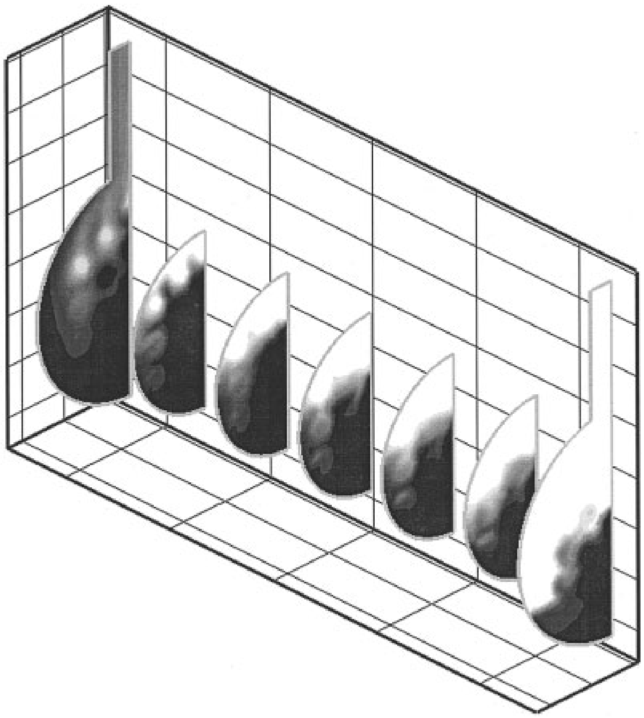

Figure 5. Concentration profiles with Darcy permeability of tabs close to positive infinity.

et al., 2000), the dialysate velocity in the upper portion of artificial kidney is higher, and urea can be transferred quickly. So the concentration in the upper portion is lower.

From the above discussion, it can be expected that if the nonporous tabs are designed to be the porous tabs with suitable Darcy permeability, the more even flow distribution of the dialysate can be obtained, and the mass-transfer performance will be increased. In fact, the mass-transfer instances discussed above are the two special conditions with the porous tabs' Darcy permeability K equal to 0 and $+\infty$, respectively [that is, the nonporous tabs could be considered as the porous tabs whose Darcy permeability runs to 0 (Figure 4), and no tabs could be considered as the porous tabs whose Darcy permeability runs to $+\infty$ (Figure 5)].

To study the effect of the porous tabs' Darcy permeability on mass transfer in detail, the clearance is simulated with Darcy permeability K decreasing from $+\infty$ to 0. When $Q_{bi} = Q_{di} =$ 400 mL/min and the Darcy permeability of the hollow fiber membrane α is equal to 1e-09 m^2, the clearance first increases slightly, and then rises sharply; after passing a maximum, the clearance falls sharply and then decreases steadily, with the porous tabs' Darcy permeability decreasing from $+\infty$ to 0. When $K \rightarrow +\infty$ (that is, without tabs), the clearance is 186.08 mL/min; when $K \rightarrow 0$ (that is, with nonporous tabs), the clearance is 227.52 mL/min. The maximal clearance is 237.45 mL/min when K is close to 1e-09 m^2, and about 4.5% higher than that with nonporous tabs (Figure 6). The result is very significant for optimization of artificial kidney design. However, the optimal Darcy permeability of the porous tabs is 1e-09 m^2, identical to the Darcy permeability of the hollow fiber. We think it is just a coincidence. In fact, many factors including the size and shape of the tabs, the dialysate inlet

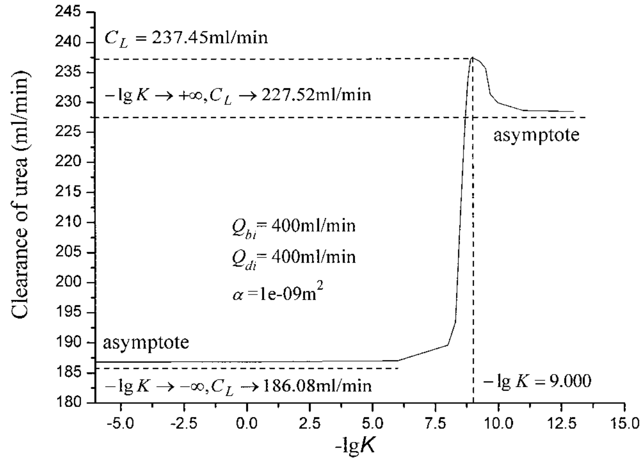

Figure 6. Variation of urea clearance with decreasing Darcy permeability of tabs.

velocity, and so on, are important to determine the optimal tab permeability. In the future, these will be discussed in detail.

Why does the clearance increase when the porous tabs' Darcy permeability is close to 1e-09 m^2? The reason can be ascertained by comparing Figure 7 with Figures 4 and 5. When the nonporous tabs are designed to be the porous tabs, a portion of the dialysate can pass directly through the porous tabs, and the rest of the dialysate goes around the distribution collar. If the porous tabs have suitable Darcy permeability, two parts of the dialysate can jointly produce a more even dialysate flow distribution. Figure 7 shows that because of the better axial flow distribution of the dialysate, urea does not congregate in

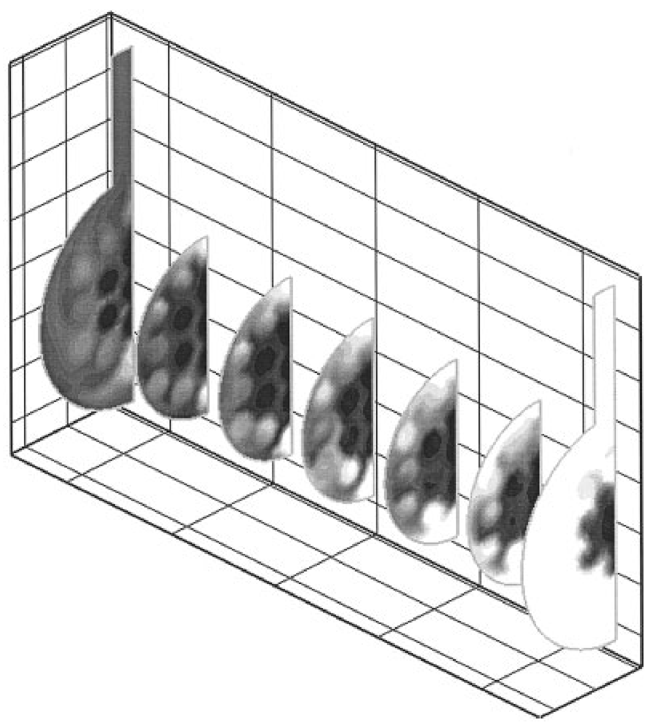

Figure 7. Concentration profiles with Darcy permeability of tabs close to 1e-09 m^2.

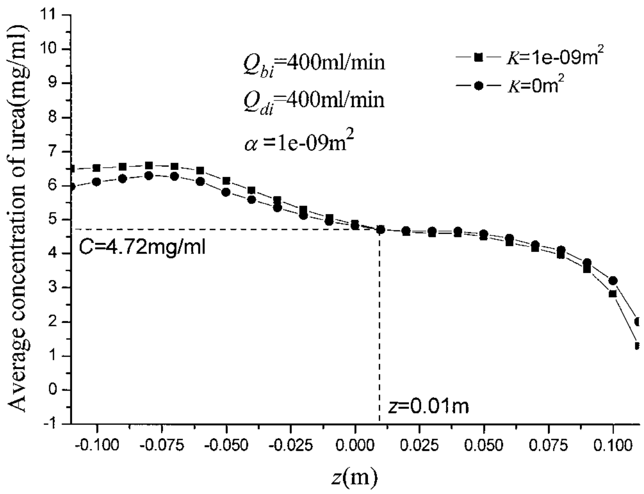

Figure 8. Comparison of cross-sectional average concentrations.

the upper or lower portion of the bundle, which leads to the better mass transfer and the higher clearance.

Figure 8 illustrates a comparison of cross-sectional average concentration values at each axial position when the porous tabs' Darcy permeability is close to 1e-09 and 0 m^2, respectively. The average concentration of urea initially increases slightly, and then decreases along the length of the module. Within the module, fluid flows preferentially in the portion of the fiber bundle close to the dialysate outlet, and urea in this region can be transported to the dialysate outlet quickly; thus, the urea concentration is lower initially. When Z increases from -0.11 to 0.01 m, the average concentration of urea with the porous tabs (1e-09 m^2) is higher than that with the nonporous tabs (0 m^2). When Z increases from 0.01 to 0.11 m, the average concentration with the nonporous tabs is higher. This tendency can also be observed by comparing Figure 4 with Figure 7. So, when the porous tabs' Darcy permeability is close to 1e-09 m^2, the urea concentration at the blood outlet is the lowest, and the mass-transfer efficiency is the best as well.

Conclusions

(1) In this article, the effect of the distribution tabs at the dialysate inlet and outlet on mass-transfer performance is investigated qualitatively by means of 3-D flow field numerical simulation. To the best of our knowledge, it is the first time to be reported in the literature.

(2) The nonporous tabs are designed to be the porous tabs. Then the variation of the artificial kidney's clearance is studied with the porous tabs' Darcy permeability decreasing from $+\infty$ to 0. The results show that the clearance first increases slightly, and then rises sharply; after arriving at a maximum, the clearance falls sharply and then decreases steadily. From the results, the optimal Darcy permeability of the porous tabs is found, corresponding to which the maximal clearance is about 4.5% higher than the current artificial kidney's clearance under the same conditions. The results are very significant for designers to improve the artificial kidney.

Acknowledgments

The help of Prof. Chen Yi-liang is gratefully acknowledged. The work is supported by the Project of Chinese Academy of Sciences on Hundreds of Scholars (2000–2003), and in part is supported by the Computation Center of Engineering Science School of USTC.

Literature Cited

Bao, L., B. Liu, and G. G. Lipscomb, "Entry Mass Transfer in Axial Flows through Randomly Packed Fiber Bundles," *AIChE J.*, **45**, 2346 (1999).

Costello, M., A. Fane, P. Hogan, and R. Schofield, "The Effect of Shell Side Hydrodynamics on the Performance of Axial Flow Hollow Fiber Modules," *J. Membr. Sci.*, **80**, 1 (1993).

Crowder, R., and E. Cussler, "Mass Transfer in Hollow-Fiber Modules with Non-uniform Hollow Fibers," *J. Membr. Sci.*, **134**, 235 (1997).

Doleček, P., and J. Cakl, "Permeate Flow in Hexagonal 19-Channel Inorganic Membrane under Filtration and Backflush Operating Modes," *J. Membr. Sci.*, **149**, 171 (1998).

Frank, A., G. G. Lipscomb, and M. Dennis, "Visualization of Concentration Fields in Hemodialyzers by Computed Tomography," *J. Membr. Sci.*, **175**, 239 (2000).

Jaffrin, M. Y., L. Ding, and J. M. Laurent, "Simultaneous Convective and Diffusive Mass Transfers in a Hemodialyzer," *J. Biomech. Eng.*, **112**, 212 (1990).

Klein, E., F. Holland, A. Donnaud, A. Lebeouf, and K. Eberle, "Diffusive and Hydraulic Permeabilities of Commercially Available Cellulosic Hemodialysis Films and Hollow Fibers," *J. Membr. Sci.*, **2**, 349 (1977).

Liao, Z. J., "Numerical and Experimental Studies of Mass Transfer in Artificial Kidney and Hemodialysis," PhD Dissertation, University of Kentucky at Lexington (2002).

Noda, I., and C. C. Gryte, "Mass Transfer in Regular Arrays of Hollow Fibers in Countercurrent Dialysis," *AIChE J.*, **25**, 113, (1979).

Wu, J., and V. Chen, "Shell-Side Mass Transfer Performance of Randomly Packed Hollow Fiber Modules," *J. Membr. Sci.*, **172**, 59, (2000).

Yang, M., and E. Cussler, "Designing Hollow-Fiber Contactors," *AIChE J.*, **32**, 1910 (1986).

Manuscript received Jan. 16, 2003, and revision received July 20, 2003.